

Article

Image Similarity Metrics Suitable for Infrared Video Stabilization During Active Wildfire Monitoring: A Comparative Analysis. Supplementary Material

M. Miguel Valero¹, Steven Verstockt², Christian Mata¹, Dan Jimenez³, LLOYD Queen⁴, Oriol Rios¹, Elsa Pastor¹ and Eulàlia Planas^{1*}

¹ Centre for Technological Risk Studies, Universitat Politècnica de Catalunya, Barcelona, Spain; mm.valero@pm.me, christian.mata@upc.edu, oriol.rios@upc.edu, elsa.pastor@upc.edu, eulalia.planas@upc.edu

² Ghent University - imec, IDLab, Ghent, Belgium; steven.verstockt@ugent.be

³ US Forest Service Rocky Mountain Research Station, Missoula Fire Sciences Lab, Missoula, MT, USA; dan.jimenez@usda.gov

⁴ National Center for Landscape Fire Analysis, University of Montana, Missoula, MT, USA; lloyd.queen@mso.umt.edu

* Correspondence: eulalia.planas@upc.edu

Received: date; Accepted: date; Published: date

1. Global sensitivity analysis

This section contains a detailed description of the results that support the GSA discussion in Sections 4.1 and 4.2 of the article. Figures 1 and 2 display the convergence of Main Effects and Total Effects estimated using original image similarity distributions as provided by similarity metrics. Figures 3 and 4 show results obtained after centering y distributions, which we found to be a critical step.

Afterwards, 5 presents individual ME and TE results for every scenario and every similarity metric considered. This figure extends the results summarized in Figure 4 of the article.

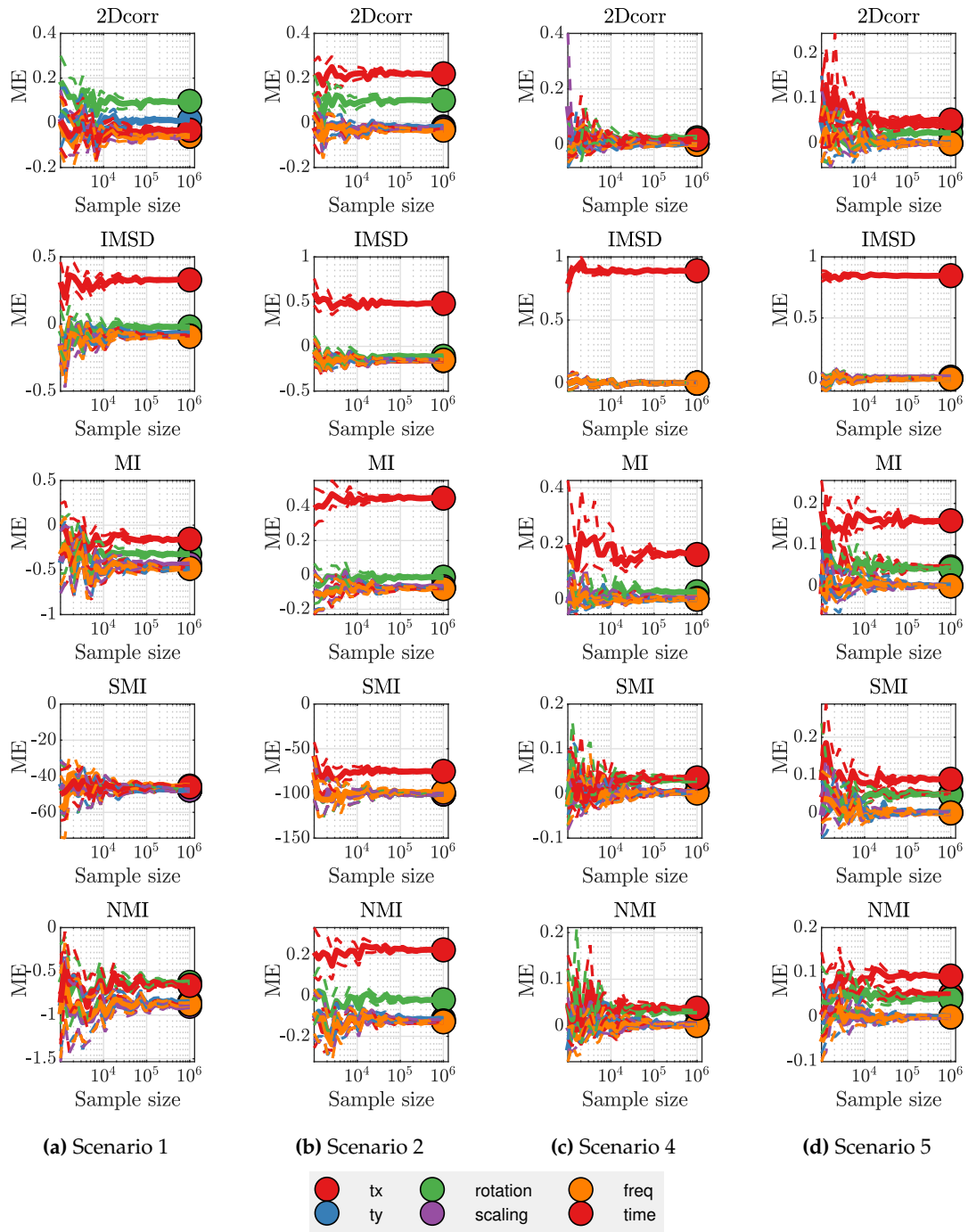


Figure 1. Variance-based global sensitivity analysis index convergence. Main Effects (ME) estimated with original model output (Y) distributions. Average values (solid lines) and confidence bounds (dashed lines) were estimated through bootstrapping with 500 resamples.

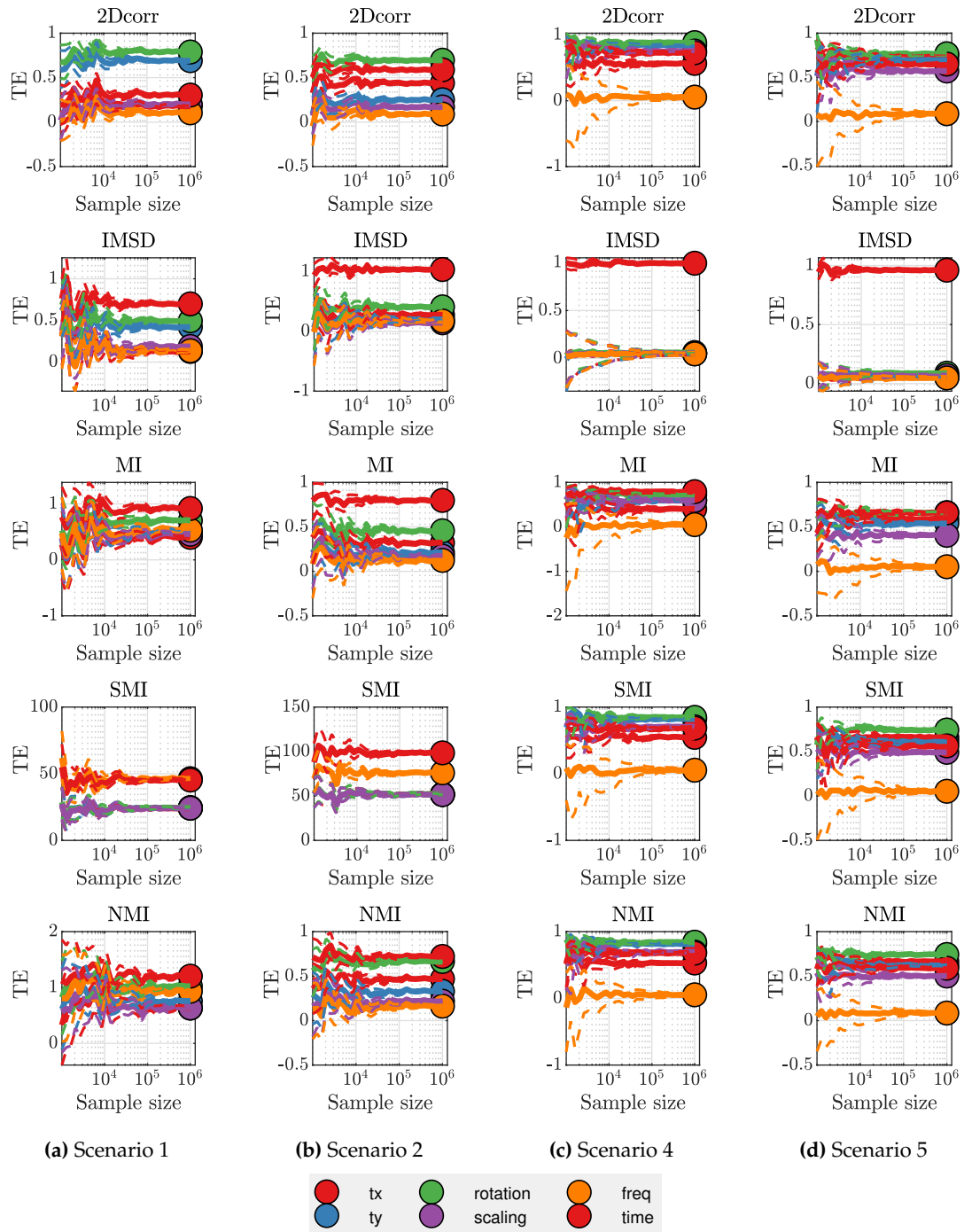


Figure 2. Variance-based global sensitivity analysis index convergence. Total Effects (TE) estimated with original model output (Y) distributions. Average values (solid lines) and confidence bounds (dashed lines) were estimated through bootstrapping with 500 resamples.

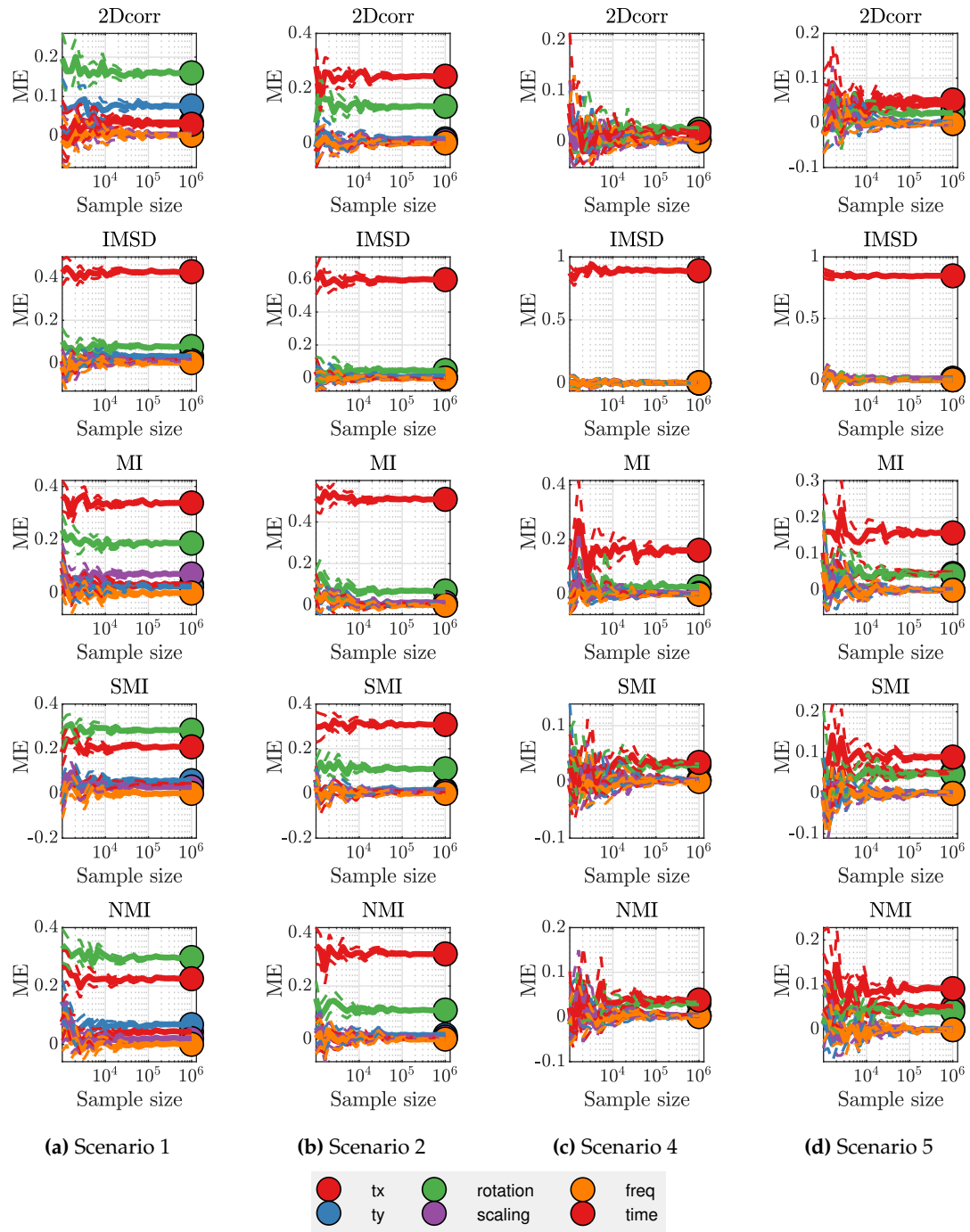


Figure 3. Variance-based global sensitivity analysis index convergence. Main Effects (ME) estimated with centred model output (Y) distributions. Average values (solid lines) and confidence bounds (dashed lines) were estimated through bootstrapping with 500 resamples.

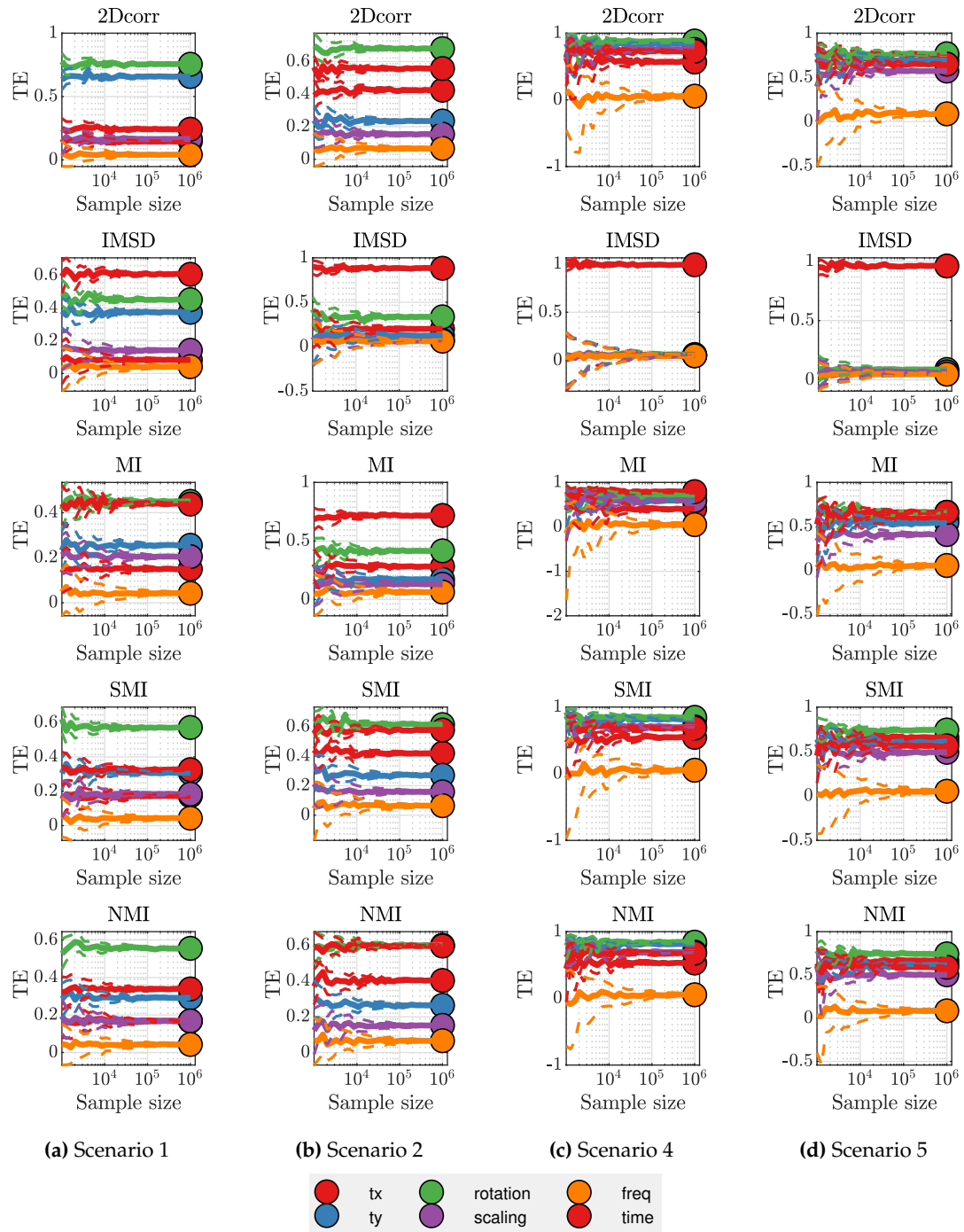


Figure 4. Variance-based global sensitivity analysis index convergence. Total Effects (TE) estimated with centred model output (Y) distributions. Average values (solid lines) and confidence bounds (dashed lines) were estimated through bootstrapping with 500 resamples.

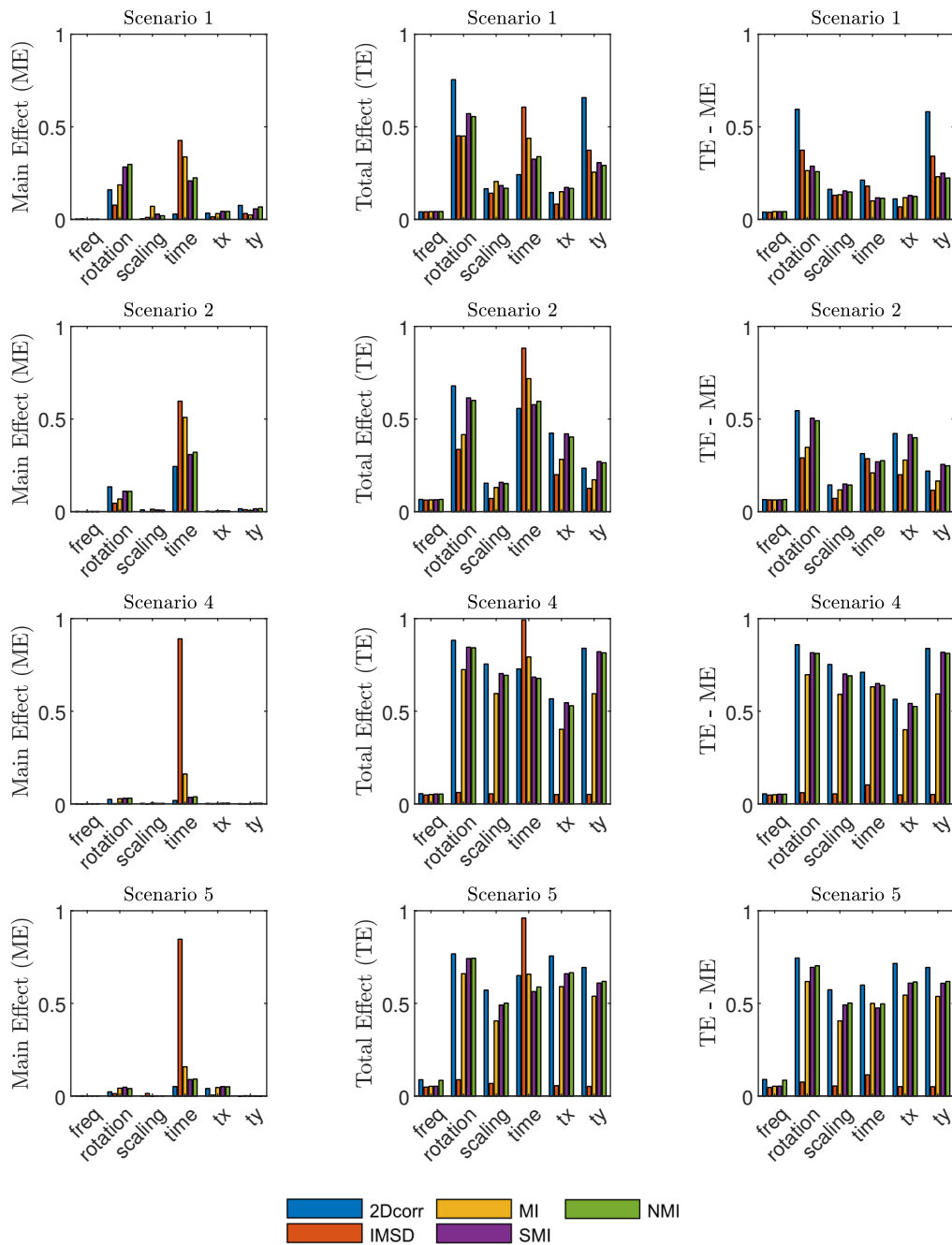


Figure 5. Global sensitivity indices of image similarity metrics to the six considered parameters. Third column displays the difference between main and total effects, indicative of the degree of parameter coupling.

2. Local sensitivity analysis

Local sensitivity analysis was applied to gain further insight into the individual response of studied image similarity metrics to different parameters. This section extends the results summarized in section 4.3 of the article.

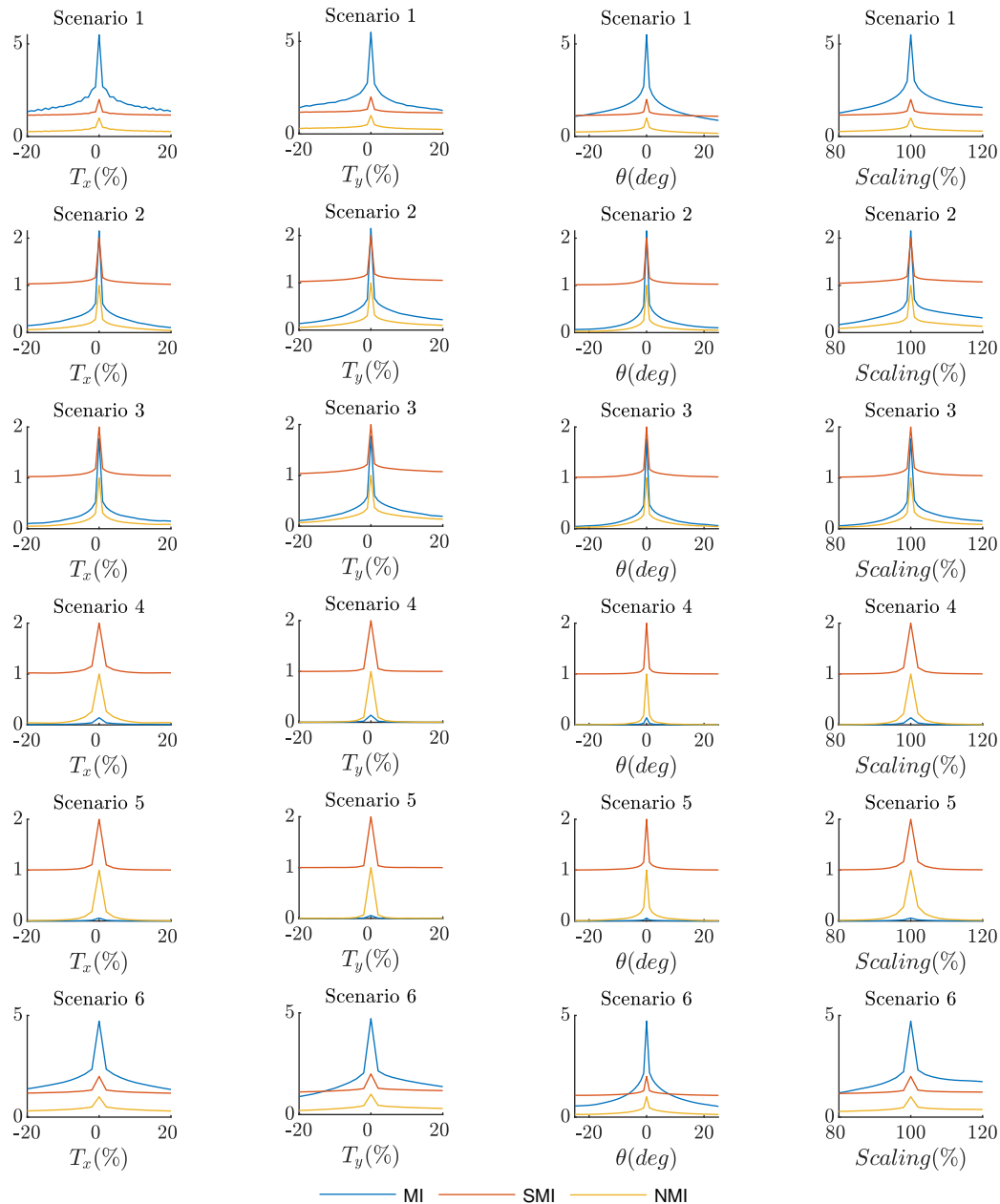


Figure 6. Local response of MI-based metrics to independent camera movement components under idealized conditions, i.e., when each video frame is compared to the stable version of itself. Values averaged along each video sequence. Camera movement components are: translation in X direction (T_x), translation in Y direction (T_y), rotation (θ) and scaling.



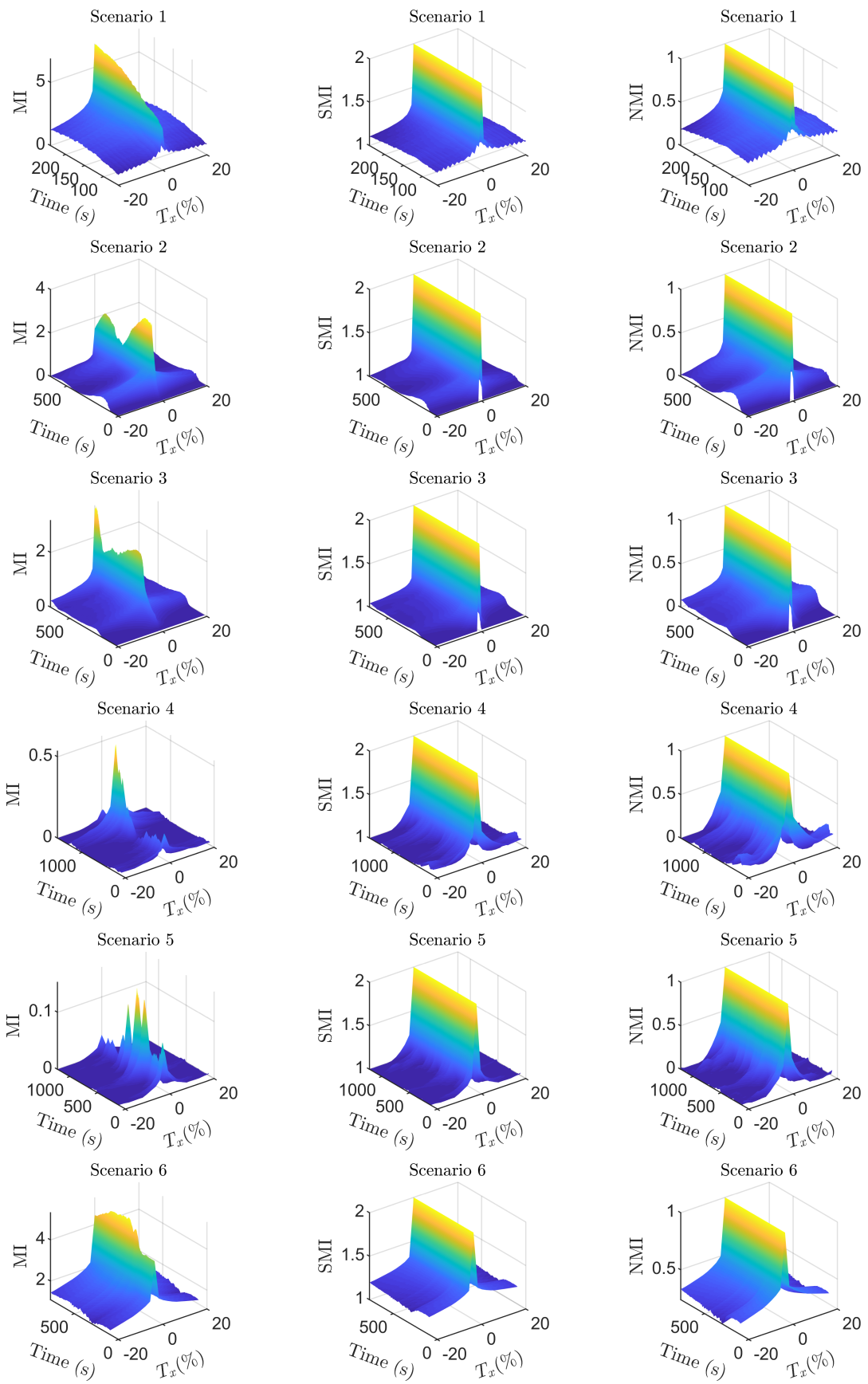


Figure 7. 3D representation of the evolution with time of MI-based metrics response to individual camera movement components under idealized conditions.

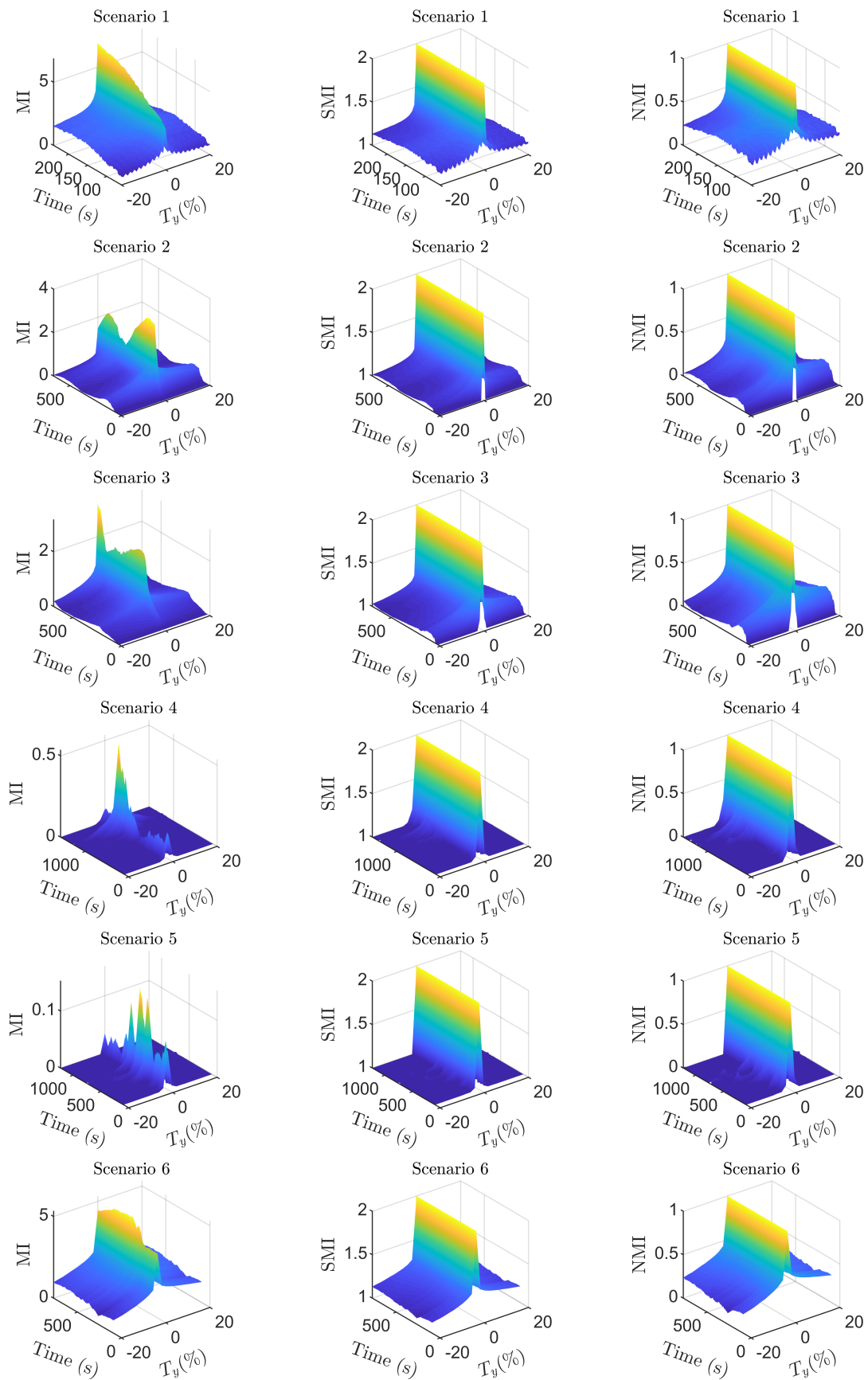


Figure 8. 3D representation of the evolution with time of MI-based metrics response to individual camera movement components under idealized conditions.

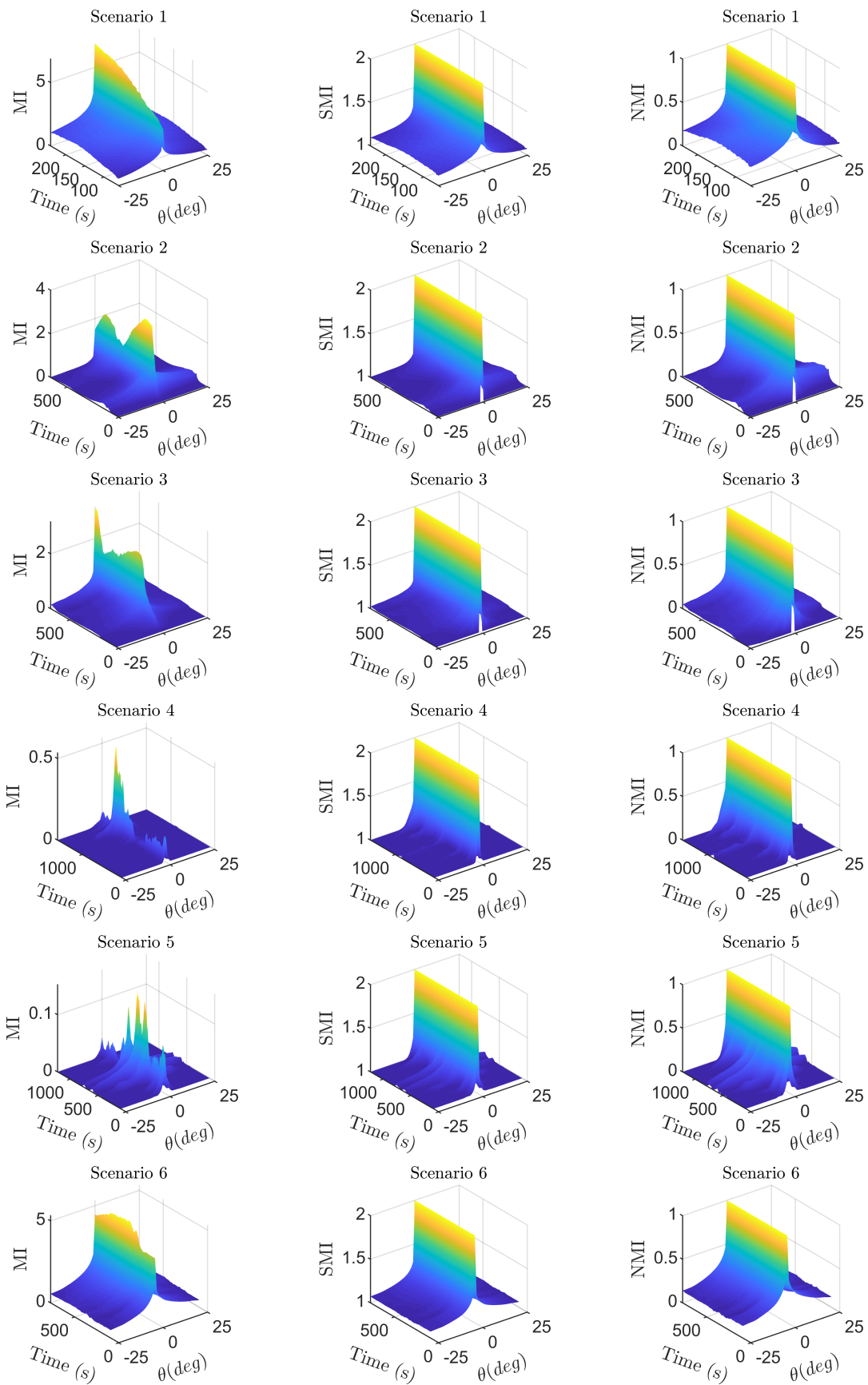


Figure 9. 3D representation of the evolution with time of MI-based metrics response to individual camera movement components under idealized conditions.

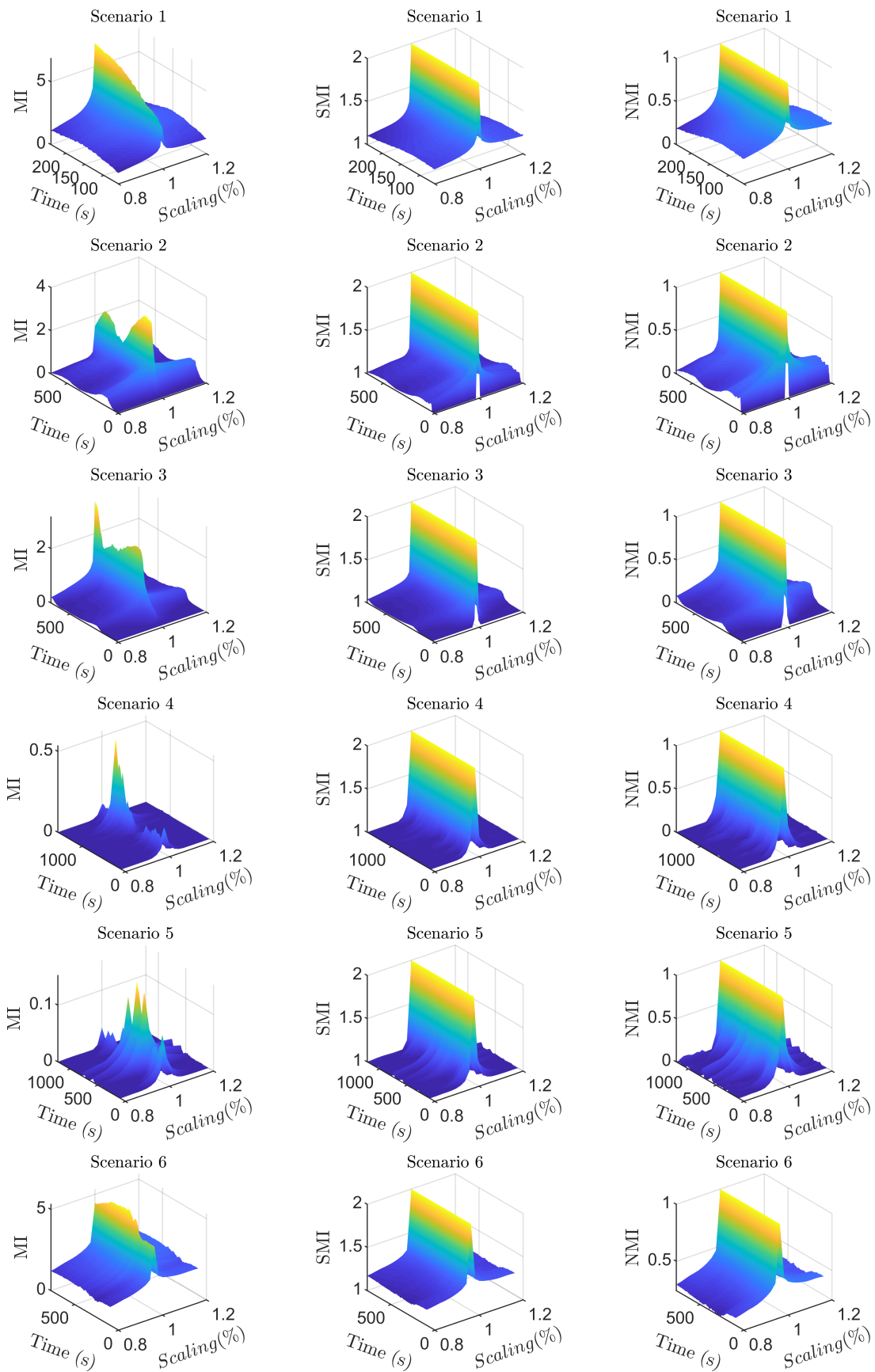


Figure 10. 3D representation of the evolution with time of MI-based metrics response to individual camera movement components under idealized conditions.

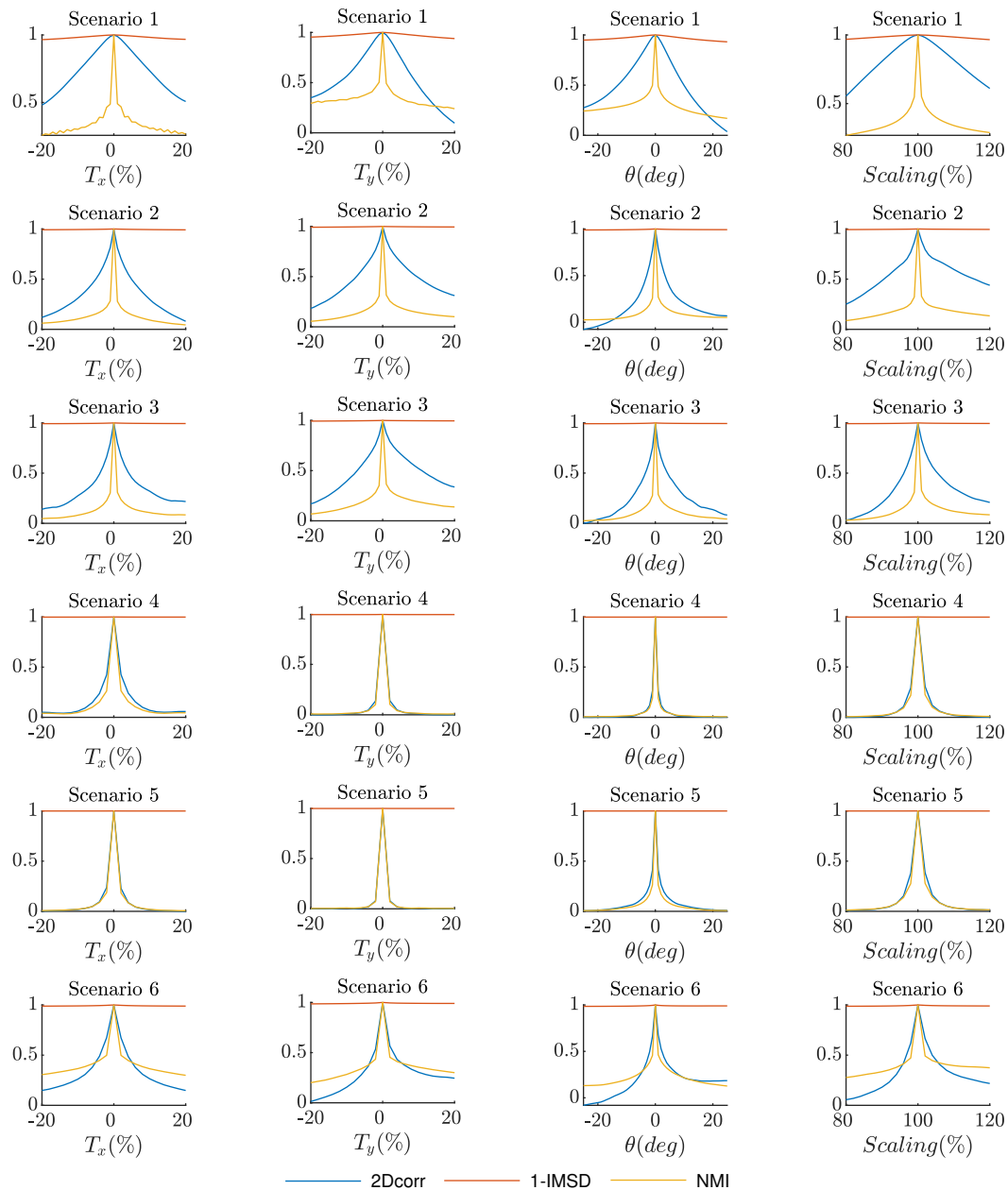


Figure 11. Metric response to independent camera movement components under idealized conditions, i.e., when each video frame is compared to the stable version of itself. Values averaged along each video sequence. Camera movement components are: translation in X direction (T_x), translation in Y direction (T_y), rotation (θ) and scaling. 1-IMSD is displayed for consistency with the rest of metrics.

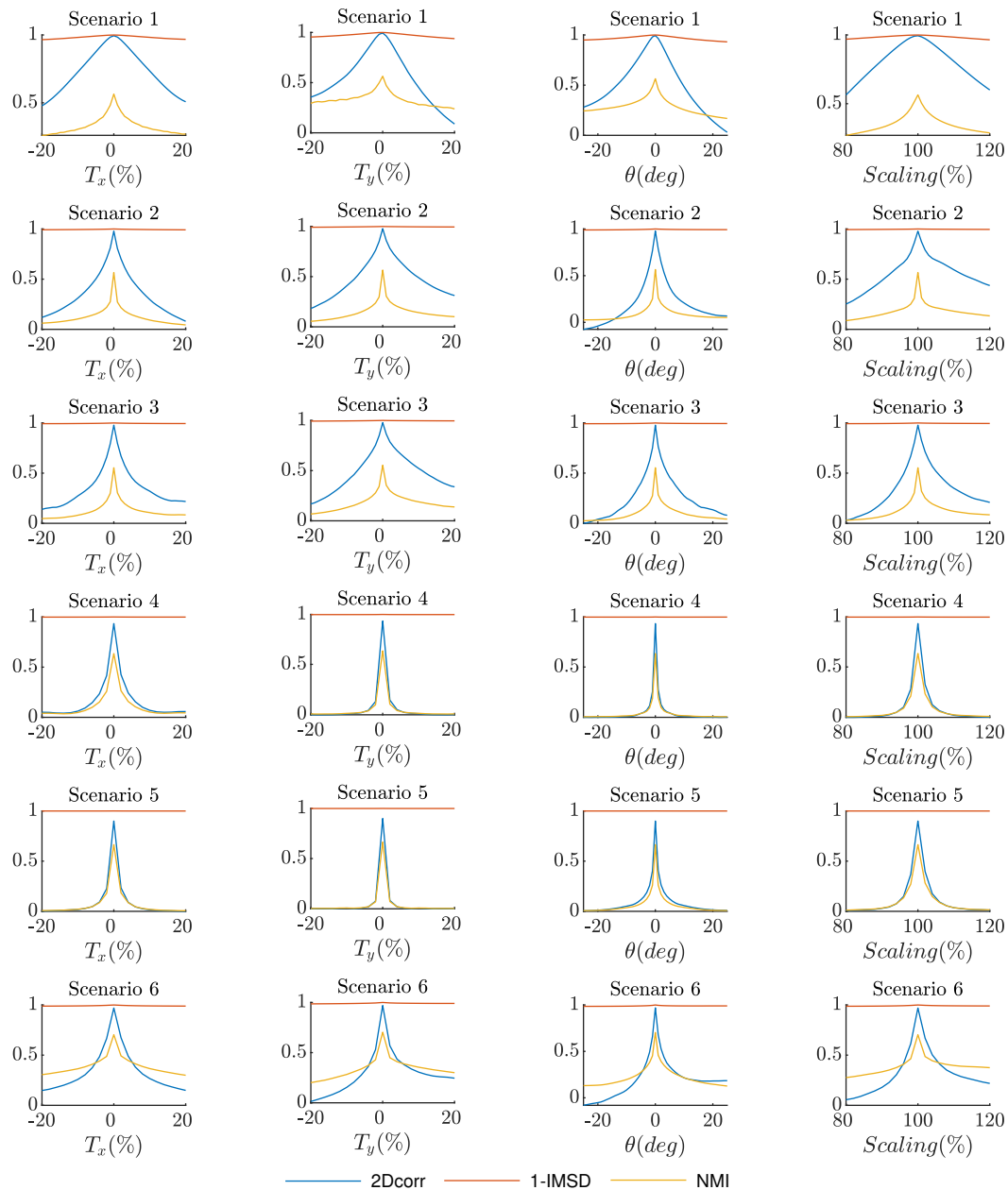


Figure 12. Metric response to independent camera movement components under real conditions, i.e., when each video frame is compared to the stable version of the previous frame. Values averaged along each video sequence. Camera movement components are: translation in X direction (T_x), translation in Y direction (T_y), rotation (θ) and scaling. 1-IMSD is displayed for consistency with the rest of metrics.

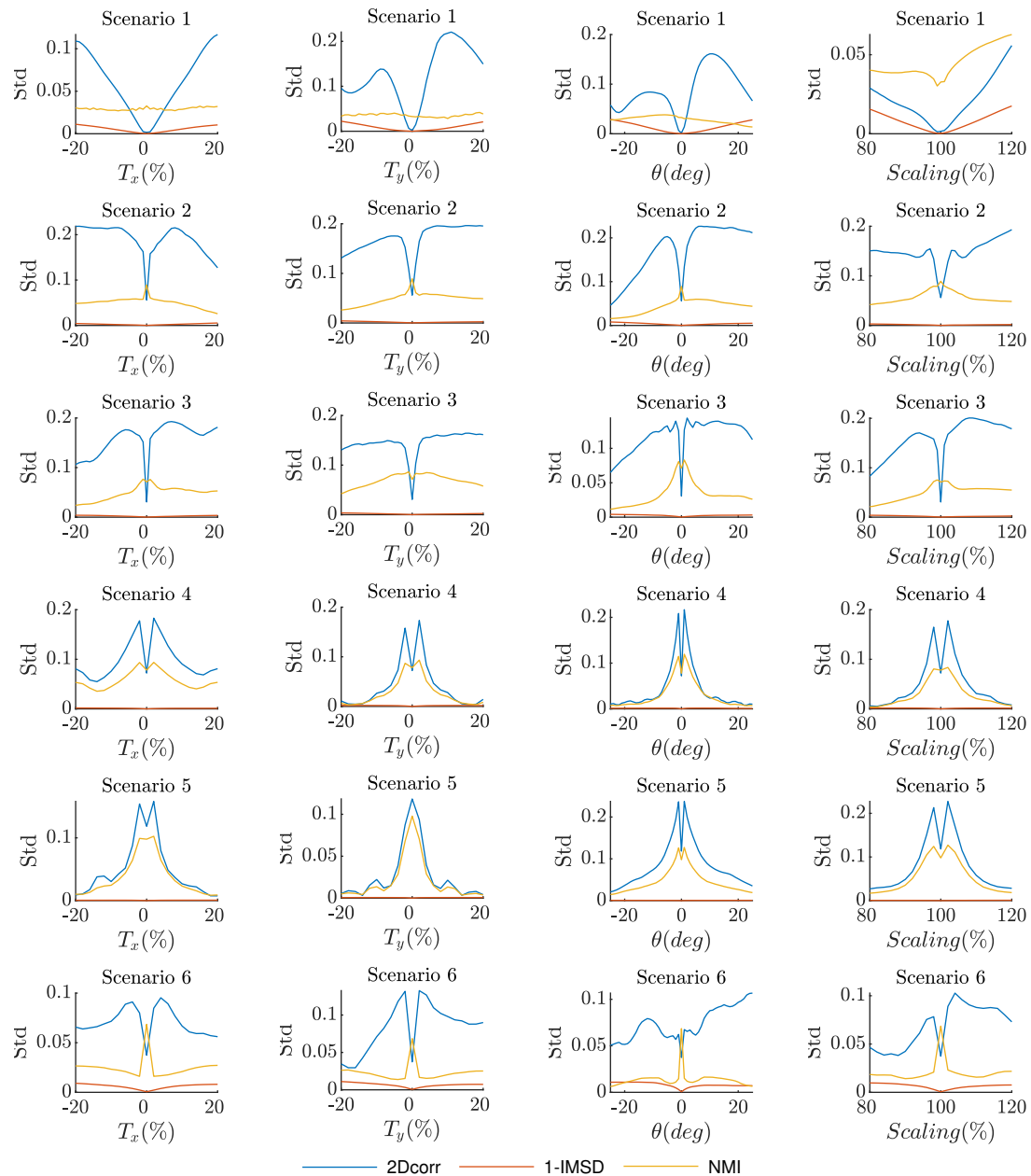


Figure 13. Metric value dispersion under real conditions, i.e., when each video frame is compared to the stable version of the previous frame. Output standard deviation, computed along each video sequence, provides a quantitative assessment of how robust each metric is in front of natural image dissimilarities and recording conditions.

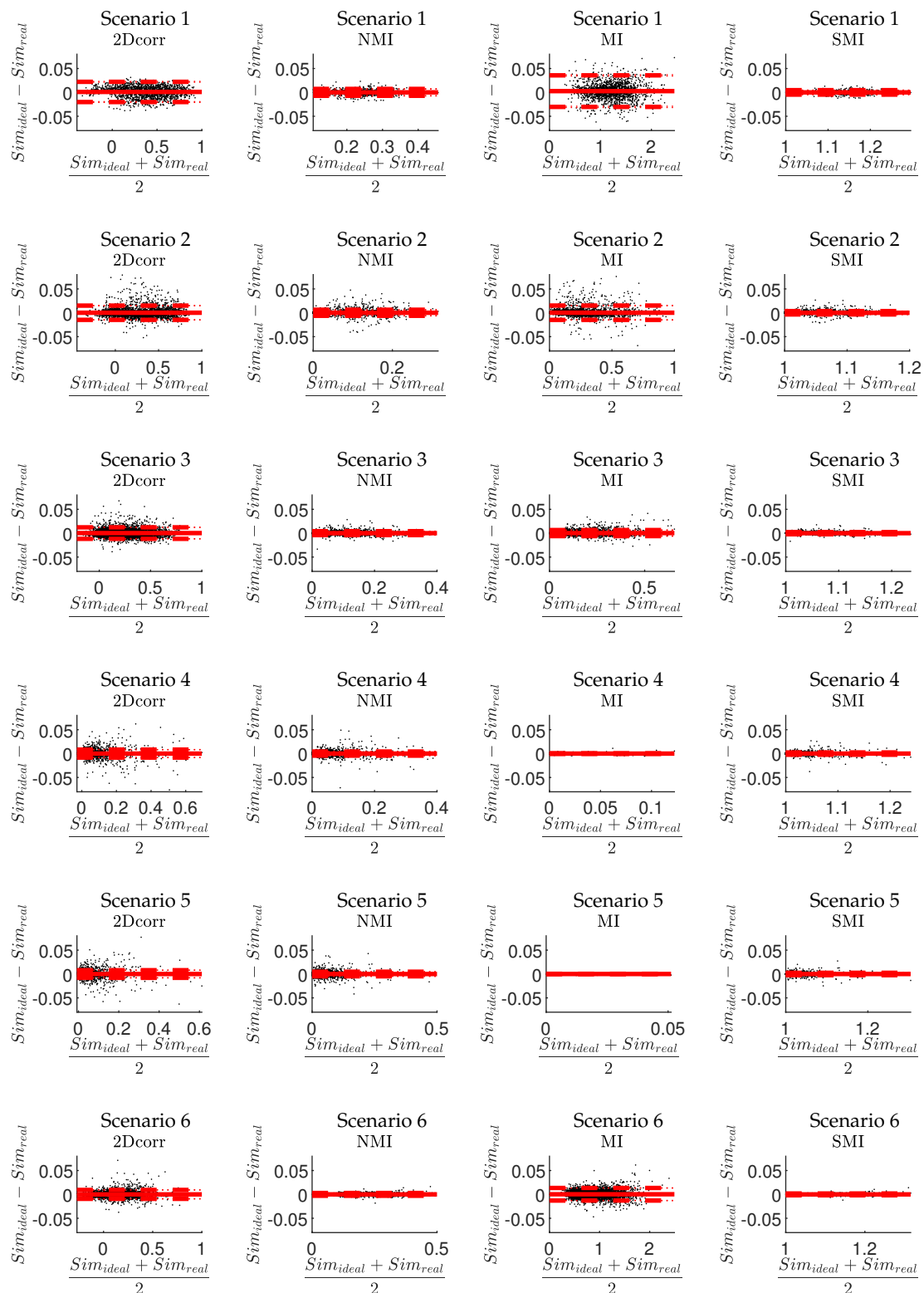


Figure 14. Bland–Altman plots comparing metric behavior under real and idealized conditions. Black dots are individual random samples along each studied scenario; red solid lines indicate mean bias; red dashed lines represent Limits of Agreement (LoA); red dotted lines represent 95% confidence intervals for estimated bias and LoA. Wide LoA are representative of significant sensitivity to changes in the reference frame used for registration.